INFORMATION
Volume 28, Number 3, pp.139-157
ISSN 1343-4500 eISSN 1344-8994

Polytope Typology C: Development of Form from Gendered 3-fold Symmetry to Bilateral Complementarity in the Polar Zonahedral Schema of the Regular and Semi-regular Polytopes by the Separation of Faces

Robert C. Meurant

Director, Institute of Traditional Studies; Adjunct Professor, Seoul National University PG College of Eng.; Exec. Director, Research and Education, Harrisco Enco • rmeurant@gmail.com • http://www.rmeurant.com/its/

Abstract

The cubic schema—considered as a 3-frequency polar zonahedron (PZ_3)—based on the separation of faces (SoF) to account for the order of the regular and semi-regular polyhedra and tessellations that I have previously presented, unveils within each symmetry class a three-fold symmetry by gender of the Primary Polytopes (PPs). This 3-fold symmetry appears remarkably pervasive, rather than an artifact of the schema, and to logically precede the bilaterality of the developed schema. Analysis of the topological relationship of proximal, like principial faces allows matrices to be developed of their relationship according to the SoF, for separation from contiguous (adjoining; d=0) to separated (adjacent; d=1), for the three gendered cases of negative (−ve), neutral (ntrl), and positive (+ve) faces. These three cases can be considered simultaneously, while horizontal rotation of the 2.5D PZ_3 schema about the primary Verticial Polytope—Great Rhomb (VP–GR) vertical axis at 2π/3 intervals can provide convenient snapshots of the corresponding pairs of the separating facial PTs (d=0 to d=1) by gender. In this paper, I reformulate my previous α|β facial convention to α|ω, to newly define α and ω as the +ve and −ve faces, respectively, of the SR (Class II: $SRCO$), and for the ntrl faces, the edges of the PL^- and PL^+ (Class II: CB and OH), respectively. Together with the (Vesica Pisces) rhombic schema of the progression of faces ($RSoF$), and the remarkable and highly regular SoF phenomenon, this PZ_3 schema, together with its rotation, provides an adequate, readily accessible modelling of the morphology of the PPs of the 3D polyhedra and 2D tessellations by class; it demonstrates the importance of the inherent three-fold symmetry of that order, in which the interplay of three tripartite genders, while constrained by the bilateral complementarities of two polar genders and one neutral, appears fundamental to objectively describing the generic structural morphology in the evolution of form of the symmetry classes of the regular and semi-regular polytopes. Finally, I consider the limitations of that underlying 3-fold order, and question whether 3-fold order might be subsumed as a 2-step differentiation of 2-fold order, to account for the form–counterform complementarity that develops between the ntrl and the other 2 genders, within the ntrl, and between the −ve and +ve genders, with respect to the PPs and their faces. The imageability of the combination of the $RSoF$ and SoF PZ_3 schema strongly recommends it to researchers and designers.

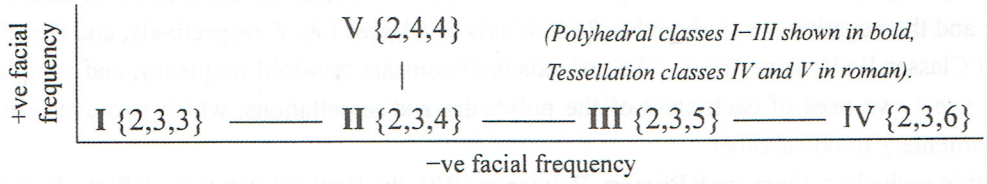

Figure 1: Symmetry Classes I–V disposed according to their +ve/−ve facial frequency.

Background via Consensus

Inspired by Critchlow [1] and the foundational work of Grünbaum and Shephard [2], the study of polyhedral morphology and the separation of faces has evolved to encompass both geometric and

combinatorial perspectives. The separation of faces in polyhedra is both a morphological phenomenon, and a subject of computational and combinatorial interest.

Recent advances in computational geometry have addressed the problem of separating a point from a polyhedron by identifying a facet or improper face using a single linear program, which is central to cutting-plane methods in integer programming, and highlights the algorithmic aspect of face separation [3]. This approach provides a practical framework to comprehend how faces can be separated or exposed in higher-dimensional polyhedra.

It has been shown from a geometric standpoint that whenever two convex polyhedra can be properly separated, a separating hyperplane may be chosen to contain a face of either polyhedron. Notably, the dimension of such an exposed face is bounded below by approximately half the larger dimension of the two polyhedra, providing insight into the structure and limitations of face separation [4].

The combinatorial structure of polyhedra, particularly the organization of their faces, has been rigorously formalized through the concept of the face lattice. This formalization demonstrates that faces form graded atomistic and coatomistic lattices, and establishes important connectivity properties of polyhedral graphs, which are essential to understand the relationships between separated faces and the overall polyhedral structure [5].

In the context of digital geometry, the problem of separating a finite set from its complement in a lattice by a polyhedron with a prescribed number of faces has been studied, with results on the decidability of such separability under certain geometric conditions [6]. This line of research extends the concept of face separation to discrete and computational settings.

Further, the classification of polyhedra with regular faces and specific vertex arrangements, such as those with rhombic vertices separated by belts of regular faces, provides a deeper understanding of how face separation can manifest in different polyhedral families [7]. Similarly, the systematic investigation of isohedra with parallelogram faces and edges in mirror planes explores the role of symmetry and face arrangement in polyhedral classification [8].

Finally, the construction and analysis of symmetric tangled Platonic polyhedra, where faces, edges, and vertices are symmetrically equivalent but the polyhedra are entangled or chiral, offer novel perspectives on the separation and interaction of faces in both mathematical and applied contexts [9].

My background and conventions

Following the conventions of my previous publications [10–22], for the regular and semiregular *PT*s, while ordering the axial frequencies as {ntrl,+ve,−ve}, Fig. 1 shows the symmetry classes on 2 primary axes of vertical +ve and horizontal −ve frequency that I recognize: Classes I–III of the polyhedra of symmetry {2,3,3}, {2,3,4}, & {2,3,5}, and Classes IV & V of the polygonal tessellations of the plane of {2,3,6} and {2,4,4} symmetry. I term the neutral (ntrl), the 2-frequency (2*f*) axis of Classes I–V; the positive (+ve), one of the two 3*f* & 4*f* axes of Classes I & V, respectively, and the 3*f* axis of Classes II–IV; and the negative (−ve), the other 3*f* & 4*f* axis of Classes I & V, respectively, and the 4*f*, 5*f*, & 6*f* axis of Classes II–V, respectively. The ntrl axis is of constant two-fold frequency, and complementary to the +ve / −ve axes of each class of the polyhedra and tessellations, which two axes are, in turn, complementary to one another.

Within each class, there are 8 Primary Polytopes (*PP*): the Verticial Polytope, VP; the Positive Polar, PL^{+}, Quasiregular, QR, and Negative Polar, PL^{-}; the Truncated Positive Polar, TP^{+}, Small Rhombic, SR, and Truncated Negative Polar, TP^{-}; and Great Rhombic, GR. These are disposed at the vertices of a rotated cubic schema, better described as a 3*f* Polar Zonahedron (PZ_3), whose main axis (one √3 diagonal of the cube) is vertical, and two enantiomorphs of the Snub Polytope ($SnbPT$), coincident at the center of the PZ_3, which are transitional forms between the QR and the SR, but in this work, are not

further discussed. Each PP is disposed according to the SoF of one of the 3 symmetry axes, proceeding from the base VP to the apex GR. This structuring is uniquely determined by the SoF (selecting one of the 2 enantiomorphs of the PZ_3). The VP (considered an abstract simplicial complex (simplex)) represents a seed PT, being of vertex (VT), with its VT^+, VT^0, and VT^- verticial faces coincident. Earlier papers describe the PPs and the schemas of the rhombic Vesica Pisces facial progression and PZ_3 PT disposition in some depth [13–22].

Principial versus pragmatic facial polytopes of the Primary Polyhedra

In considering the surface polytopes of the PPs (or PTs, one being verticial), I draw a critical distinction between the *principial* facial polytopes, and the *pragmatic* (contingent/incidental) facial polytopes. The pragmatic facial polytopes are those commonly recognized, e.g., the 6 SQ & 8 TR faces, 12 vertices, and 24 edges of the QR CO. But the principial facial PTs are limited to those that are regularly disposed on the symmetry axes of that class, so in this case, 6 −ve RSs, 12 ntrl VTs, & 8 +ve RTs; therefore, the edges of the CO, which do not lie on the symmetry axes, are pragmatic, but not principial—they rather arise incidentally as the shared edge of contiguous RS & RT faces. But all 3 gendered VTs of VP, the −ve, ntrl, & +ve VTs of OH, CO, & CB, the ntrl EGs of OH & CB, and one set of the EGs of TO & TC, are considered principial.

The principial facial polytopes then form an inner harmony to the facial polytopes, in some sense a deeper formal structure to the PPs, akin to the checkerboard pattern lying within the square array, or the multi-frequency square arrays within the basic unit square array. Considering that a significant number of vertices of the PPs are *not* regularly disposed on the symmetry axes (e.g., all vertices of the GR, SR, TO, and TC), the regularities around those pragmatic vertices are likely of lesser significance in appreciating the structural morphology of these PTs; their axes through the PT center are not significant in terms of the PT symmetry (the common edge of ntrl pairs of TR faces is perpendicular to the neutral axis of the Snub PT).

Transition from the α↔β convention to the α↔ω convention

Previously, I assigned α↔β to distinguish the two level 1 facial forms for each gender that are duals, based on the α form characterizing the +ve & −ve axes of the PL^+ & PL^-, and the β form their −ve axes, respectively; with the α & β characterizing the ntrl axes of the PL^+ & PL^-. The generic rhombic schema, shown in Fig. 2, was previously developed into the rhombic schema of the progression of faces ($RSoF$), shown in Fig. 3.

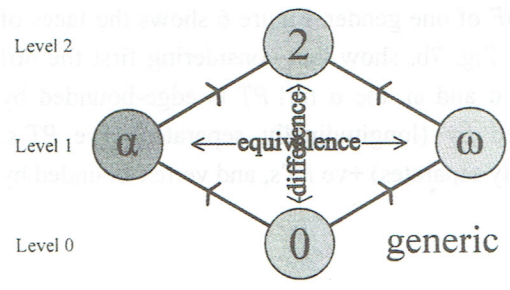

Figure 2: Generic Vesica Pisces rhombic schema: on the −ve, ntrl, or +ve axis. Here, **0** represents the 0° VT (−/0/+ve verticial face); **α** and **β** represent the dual 1° forms of the primary polygonal face; **2** represents the fully developed 2° form of that face (Class II: OG, SQ, or HX).

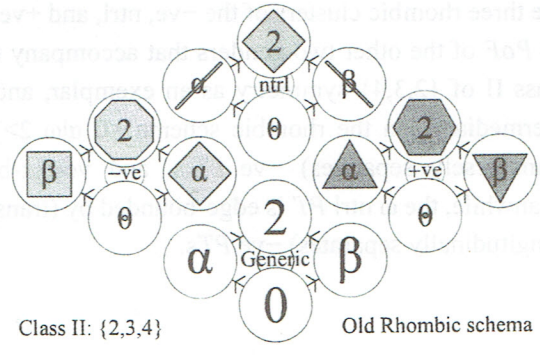

Figure 3: Class II level 0, 1 (α|β), & 2 faces by the old convention. In Class II, **α** & **β** are represented by the 1° forms: SQ, EG, or TR, and their duals RS, EG^+, or RT. Level 0 VTs as dots; ntrl **α|β** edges, 2-gons; bottom, generic; left, −ve, top, ntrl; right, +ve.

That analysis eventually led to inconsistency in terms of the finer grain symmetry of the developmental sequences of the rhombic schema, so I now use the convention shown in Figs. 4 and 5 below:

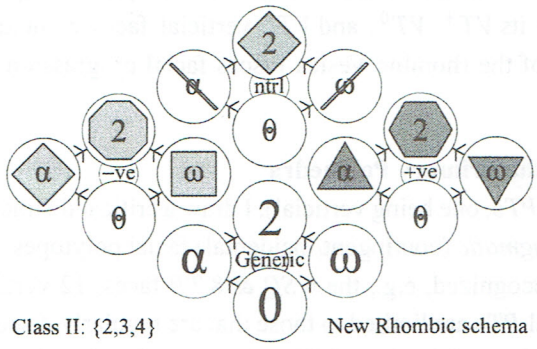

Class II: {2,3,4} New Rhombic schema

Figure 4: Class II level 0, 1 (α|ω), & 2 facial types by the new convention. Bottom, Generic; left, −ve, top, ntrl; right, +ve; level 0 *VT*s shown as dots, ntrl α|ω edges as 2-gons. The −ve α|ω faces become those of the *CO* | *CB*, respectively, as the faces of the −ve rhomb are reflected to express the bilateral symmetry of the whole, and the ntrl α|ω faces are reflected from the α|β case.

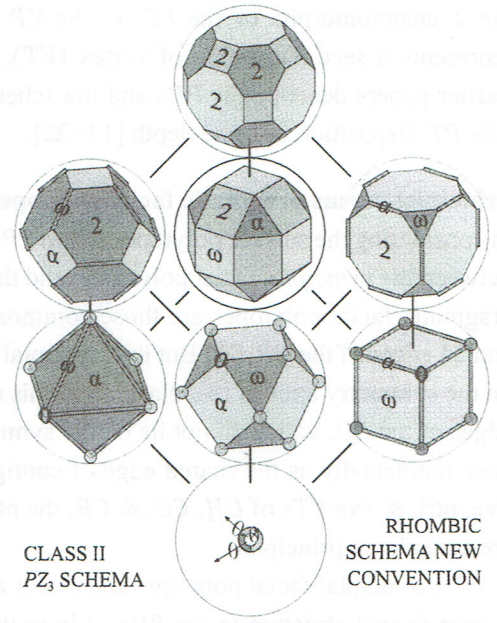

(Positive, dark; Neutral, mid-; Negative, light grey).

Figure 5: New Class II Rhombic Schema of level 0, 1 (α|ω), and 2 faces. *VP*, small tri-grey circle with 0-axes; *VT*s, small circles by gender; ntrl α|ω edges, 2-gons. The −ve α & ω faces have switched positions *(cf.* Fig. 2); −ve α & ω faces are now those of the *CO* & *CB*; ntrl α & ω faces have switched to the edges (2-gons) of the *CB* & *OH*, respectively. Overall, the α↔ω dialectic replaces the α↔β.

Accordingly, for the rest of this paper, I rename the two level 1 faces (α & β) as the duality α↔ω, shown in Fig. 4 above, and reassign them on the basis of the +ve & −ve faces of the *SR* and *QR*, as in Fig. 5, so that they properly reflect the presumed morphology of the 'opposition of oppositions' or 'duality of dualities'. Without loss of generality, the α|ω labels are first applied to the +ve & −ve faces of the *SR* and *QR*, and thus to the −ve & +ve faces of the *QR* and *SR*, as in Fig. 5. The ntrl level 1 α & ω labels are now assigned to the faces (2*f* edges) of the PL^- and PL^+, respectively. These changes allow the finer grain of the four strata of the PZ_3 schema to be consistently represented, with each facial type 0, α, ω, & 2 in contiguous and separated status. Except for *VP* & *GR*, each *PP* has different facial type by axis. The three rhombic clusters of the −ve, ntrl, and +ve genders share the same generic form, and delineate the *PoF* of the other two genders that accompany the *SoF* of one gender. Figure 6 shows the faces of Class II of {2,3,4} symmetry as an exemplar, and with Fig. 7b, show that considering first the ntrl intermediary (on the rhombic schema <0 α|ω 2>) *PT*s α and ω, the α ntrl *PT* is edge-bounded by (transversely separates) −ve *PT* s, and vertex-bounded by (longitudinally separates) +ve *PT* s; meanwhile, the ω ntrl *PT* is edge-bounded by (transversely separates) +ve *PT*s, and vertex-bounded by (longitudinally separates) −ve *PT*s.

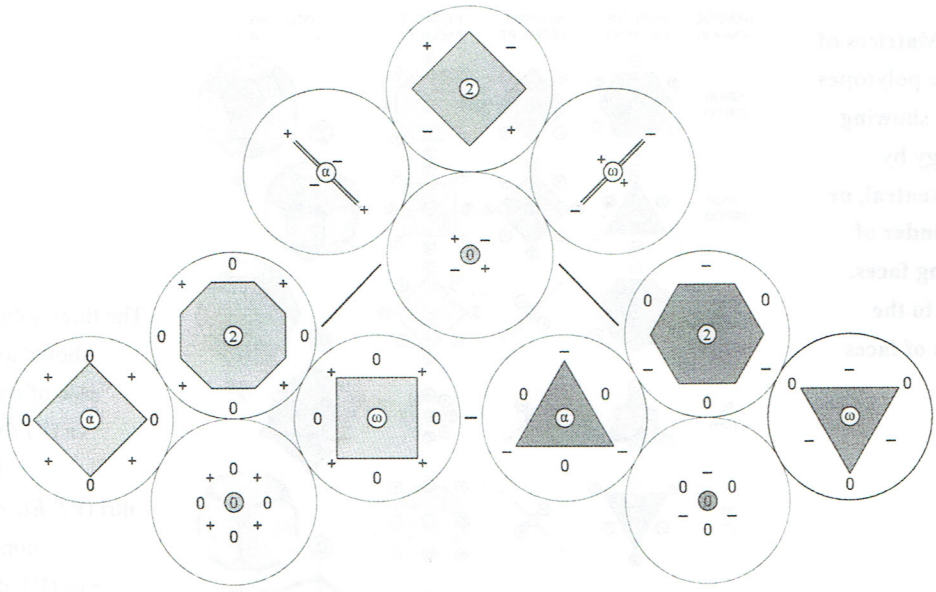

Figure 6: Rhombic schemas of the −ve, ntrl, & +ve faces of Class II. These show the alternation by gender of circumferential faces around each gendered face for schematic levels 0, 1= α|ω, & 2. *VT*s of the *VP* are shown as small grey circles, ntrl *EG*s (α & ω) as 2-gons; for each of the three genders, the α|ω faces are duals.

The pervasiveness of 3-fold symmetry in the PZ_3 Schema of the *PP*s by facial topology

Figure 7 shows the matrices of the surface polytopes of Class II as exemplar, revealing the topology by gender of neighboring faces, attending to the separation of −ve, ntrl, and +ve faces, respectively. For each of the three genders, each face appears twice, as contiguous or separated (d=0 or 1), as delineated in the respective right-most column. For this purpose, certain vertices (VP^{-0+}, OH^{-}, CO^{0}, CB^{+}), or edges (VP^{-0+}, OH^{-}, CB^{+}, TO^{0}, TC^{0}), are considered faces of zero extent or width, shown as small circles and 2-gons, respectively, where the face they represent is principial. The three subfigures are shown together (Fig. 7; lower left, upper center, lower right) for convenient comparison.

As expected from the pattern of symmetry axes, each face of a particular gender of each of the eight *PT*s is characterized by the same necklace of surrounding contiguous polytopes that alternate in gender between the other two genders. In terms of principial faces, each gendered axis is surrounded by alternating axes of the other two genders, there being no distinction between ntrl (0) and polar (−,+) axes—the three genders appear to form a tripartite system.

The respective right-most column shows the separation of faces transformation of each pair of corresponding *PT*s for that particular −ve, ntrl, or +ve gender. In each case, contiguous pairs of verticial, edge, or polygonal face separate by unit (edge length) distance. For a particular gender, the same face occurs twice in the class; first as the lower contiguous case, which pairs initially share either vertex or edge; and then as the higher separated case, in which pairs are separated by unit distance. This phenomenon is traced in detail in my previous work [19–22], and forms the basis for the arrangement of the cubic & PZ_3 schema (in 1 of its enantiomorphs).

By considering the principial, rather than the pragmatic, surface *PT*s, it becomes clear firstly, that each progression of contiguous gendered faces about a reference surface polytope alternates genders of the other two genders; so for example, around the −ve SQ face of the $PL^{-}\ CB$, +ve VT^{+} 'faces' and ntrl EG^{0}s (2-gons) alternate. This means that the various patterns of gender are subdividable into triangular components of the three genders, which alternate in chirality, so for the −ve face, $\widehat{0-+}$ and $\widehat{+-0}$; for the ntrl face, $\widehat{-0+}$ and $\widehat{+0-}$; and for the +ve face, $\widehat{-+0}$ and $\widehat{0+-}$. The VP faces may be considered to be latent, of zero extent.

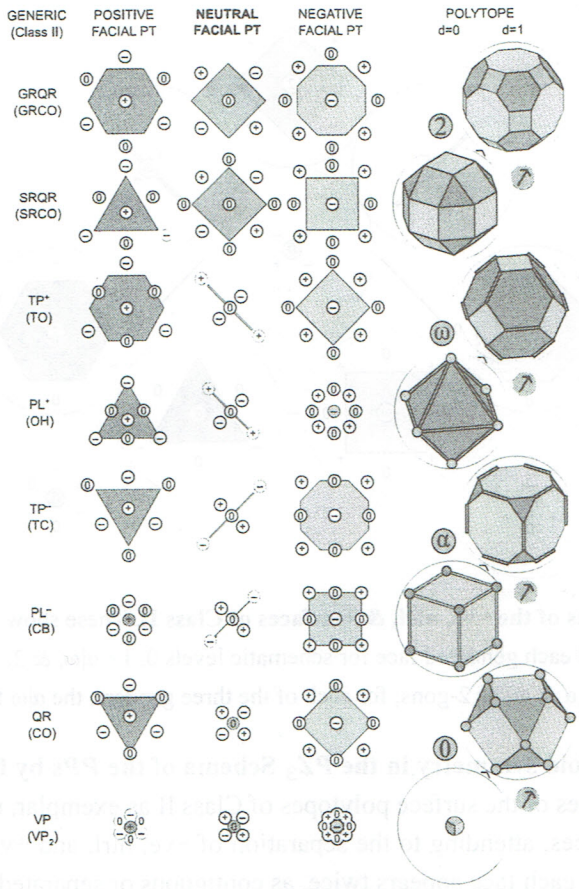

Figure 7: Matrices of the surface polytopes of Class II showing the topology by negative, neutral, or positive gender of neighboring faces, according to the separation of faces.

The three subfigures are shown together for ease of comparison. −ve (VT/light grey), lower left; ntrl (VT/EG/mid-grey), upper central; +ve (VT/dark grey), lower right. For each subfigure by gender, each face appears twice in the right-most column, from contiguous (d=0), to SoF separated (d=1).

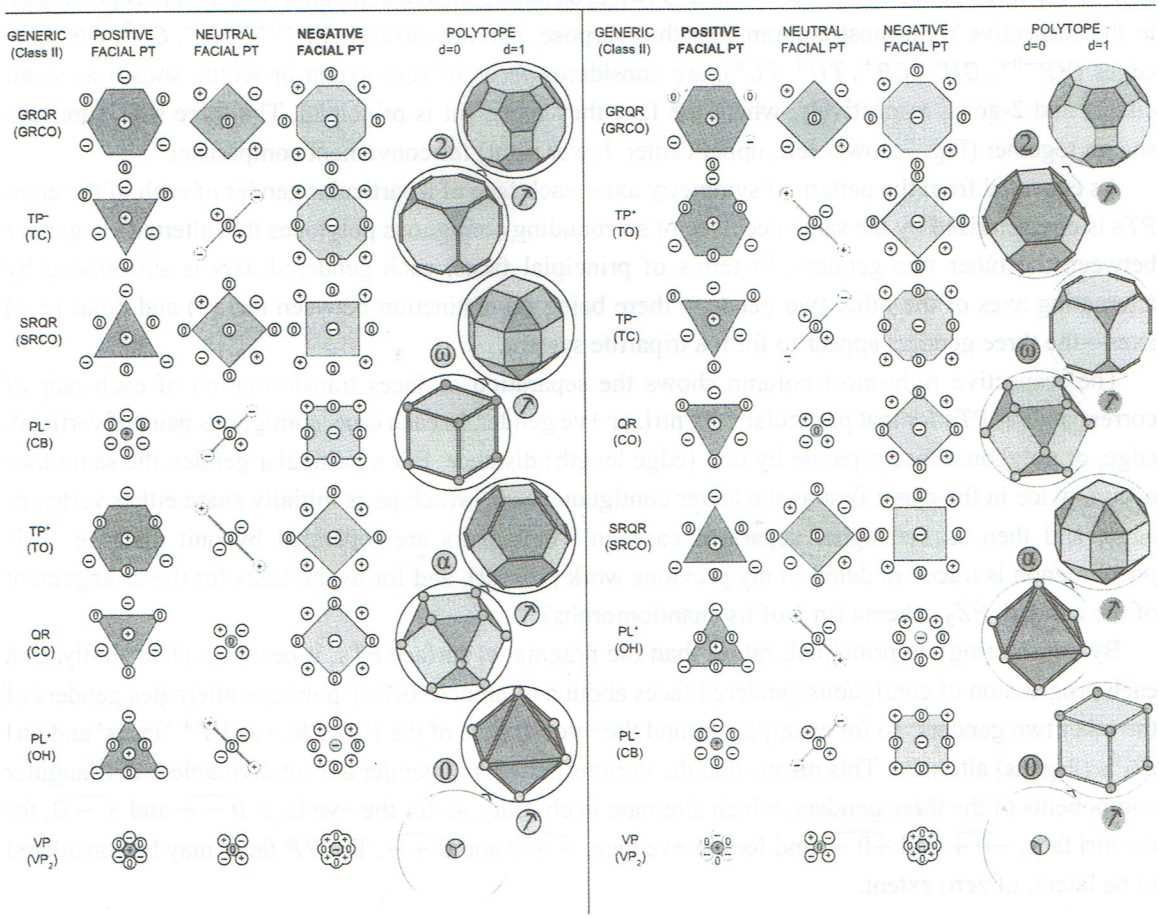

The differentiation into and interplay of the three genders therefore seems fundamental to the form and interrelation of the polyhedra. However, the ntrl has particular qualities that differentiate it from the −ve and +ve, that go beyond the unique character of 2*f* symmetry; it seems to be self-dual, and appears to generate internally two kinds of ntrl α and ω elements; by contrast, −ve and +ve elements are dual *internally* within the 2D facial level of the α↔ω duality, and *externally* at firstly, the dual +ve↔−ve correspondence of faces (at all 3 levels (0, α|ω, and 2) of the rhombic schema), and finally, at the polar 3D polyhedra levels of the dual $OH \leftrightarrow CB$ and form–counterform $TO \leftrightarrow TC$. The bilateral complementarity of the PZ_3 schema imposes an undeniable facticity on what appears to be a primordial 3-fold symmetry. The 2-fold form–counterform complementary nature of the polyhedral order seems to be in cosmogonic terms, in the emergence of form from potential, a later developmental constraint, almost a geological intrusion on a purer 3-fold perfect symmetry of 3 tripartite genders. Simultaneously, there is a creative tension between the two that stimulates the imagination; the 2-fold division seems more prosaic; the 3-fold more subline. The two-fold is profane; but the three-fold transcendent.

Thus the bilateral differentiation by +ve/−ve gender, and by α | ω face, conditions the strong three-fold order: at the 3D polyhedral level, the duality for the +ve and −ve *PT*s applies to the polar OH—CB, and in the form–counterform complementarity TO—TC, while at the 2D facial level, each pair of −ve, ntrl, and +ve α—ω polytopes are duals. These oppositions are regarded as complementarities that are external for the +ve and −ve genders, and internal for the ntrl gender; and can be generalized to the polar pairs VP–$GRCO$, OH–TC, CO–$SRCO$, and CB–TO.

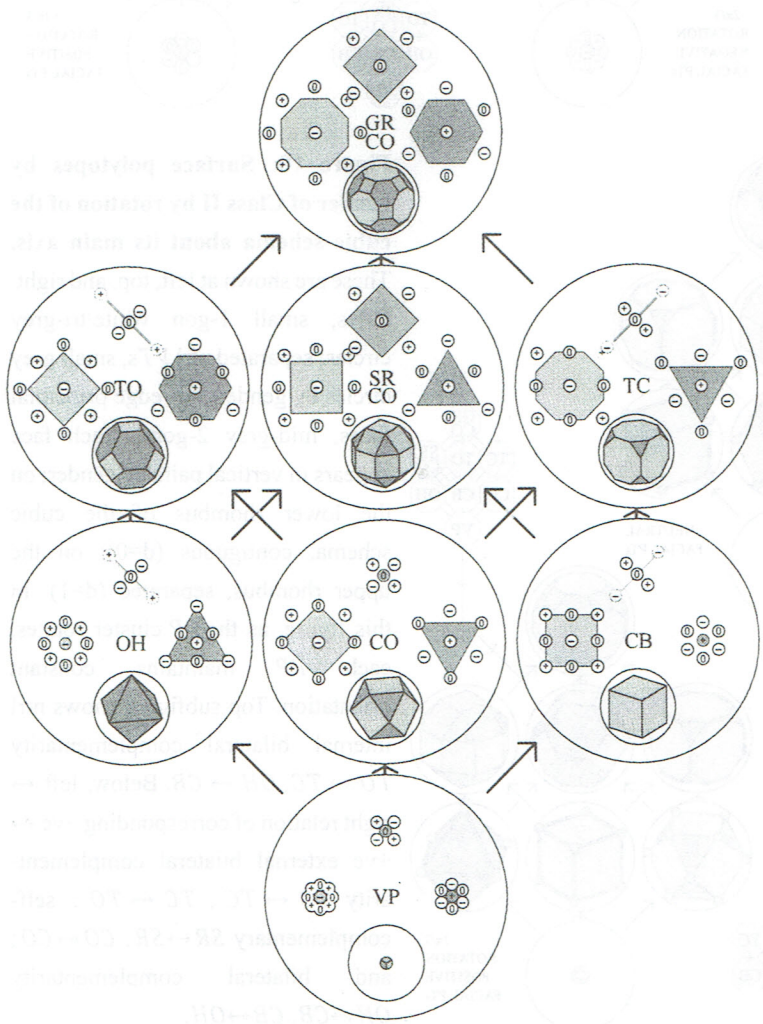

Figure 8: Surface polytopes by gender of Class II showing the disposition by gender of neighboring faces. As expected, within each gender, the formal pattern of neighboring genders is identical, with each face seen twice, as contiguous (d=0) or separated (d=1). The cubic PZ_3 schema devolves into two rhombic schemas: a lower rhomb representing d=0, and an upper rhomb, d=1. $<VP \rightarrow OH|CB \rightarrow SRCO>$ of the lower, contracted rhomb is precisely reflected in the $<CO \rightarrow TO|TC \rightarrow GRCO>$ of the upper, expanded rhomb; all classes share the generic $<VP \rightarrow PL^{+}|PL^{-} \rightarrow SR> \leftrightarrow <QR \rightarrow TP^{+}|TP^{-} \rightarrow GR>$ dialectic.

Figure 9: Surface polytopes by gender of Class II show the disposition by gender of neighboring faces. Rotation of the cubic 2.5D schema of PPs by $2\pi/3$ about the vertical $\sqrt{3}$ axis shows snapshots of pairs of corresponding faces, with contiguous (d=0) below, separated (d=1) vertically above. −ve, left; ntrl, top; +ve, right. (At each rotation of the PZ_3 cluster of PPs, each component PP also individually rotates in parallel by the same angle about the same axis to present its appropriate face and orientation).

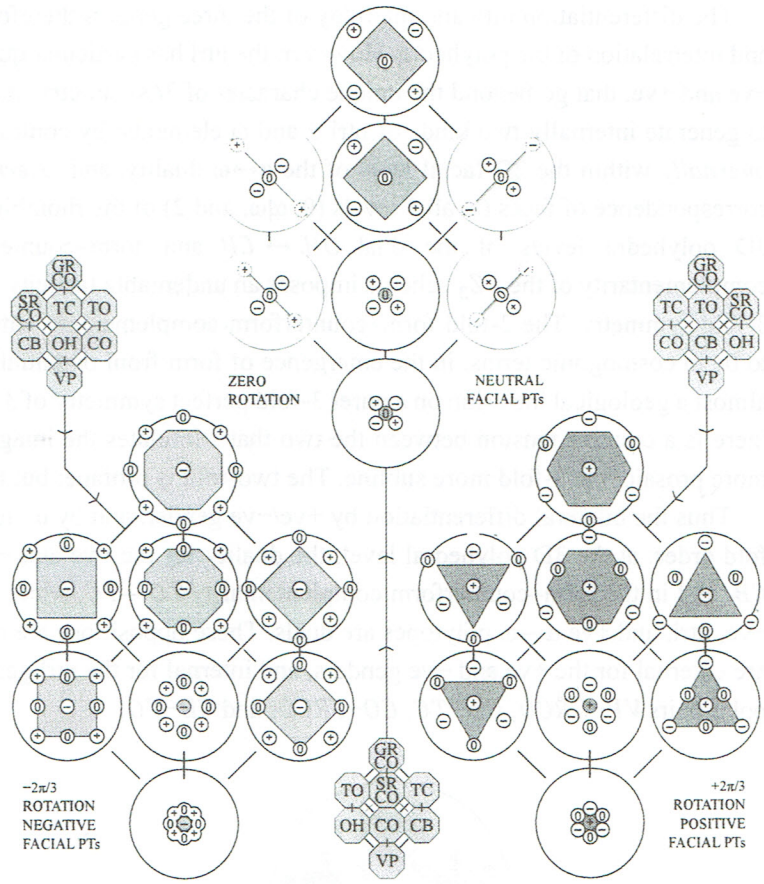

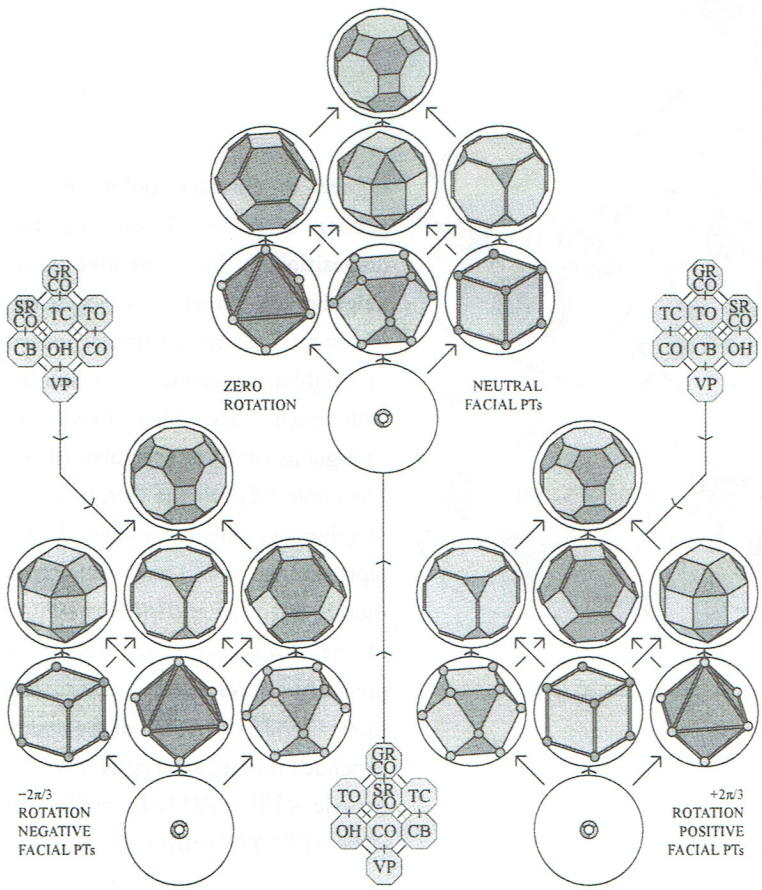

Figure 10: Surface polytopes by gender of Class II by rotation of the cubic schema about its main axis. These are shown at left, top, and right. VP s, small 1-gon white/tri-grey circles; separated ntrl VTs, small grey circles by gender; ntrl edge principial faces, mid-grey 2-gons. Each face appears in vertical pairs by gender; on the lower rhombus of the cubic schema, contiguous (d=0); on the upper rhombus, separated (d=1). In this figure, as the PP cluster rotates, each PP maintains constant orientation. Top subfigure shows ntrl internal bilateral complementarity $TO \leftrightarrow TC$, $OH \leftrightarrow CB$. Below, left ↔ right relation of corresponding −ve ↔ +ve external bilateral complementarity $TO \leftrightarrow TC$, $TC \leftrightarrow TO$; self-complementary $SR \leftrightarrow SR$, $CO \leftrightarrow CO$; and bilateral complementarity $OH \leftrightarrow CB$, $CB \leftrightarrow OH$.

Figure 9 shows the Class II disposition by gender of the principial surface polytopes. Each cubic schema devolves into two rhombic schemas: a lower rhomb of contiguous faces (d=0), and an upper rhomb of separated faces (d=1). Within each gender, each face occurs twice, contiguous & separated for d=0 & 1, according to the *SoF* previously described [22: fig. 1].

Figure 10 confirms the regularity of the correspondence of facial pairs according to the separation of faces from contiguous (d=0) to separated (d=1), rotating the cubic schema of *PP*s about its main vertical axis from left to right at $-2\pi/3$, 0, and $+2\pi/3$ for −ve, ntrl, and +ve faces, respectively (*PP* positions vary by schema, except for the *GR & VP*). As previously observed [21], the cubic schema of polyhedra suggests the cosmogony of the *PP*s within a class by the separation of faces from *PT* to *PT*: the initial eruption of the absolute into these facial forms seemingly so intense that they must push away from one another, to soften their forms, expanding to full-bodied existence; but in holistic fashion within tight, constrained 3*f* symmetry.

The PZ_3 has 3 zones of sheaths of parallel edges/linkages; for example, in the neutral subfigure (top) of Fig. 9 above, for the separation of faces, the 'vertical' sheath of edges/linkages in this figure denotes the separation of neutral faces; the ascending right sheath denotes the separation of +ve faces, while the ascending left sheath denotes the separation of −ve faces. Meanwhile, the rotations of the three subfigures at left, top, and bottom show for the 'vertical' linkages, the separation of the −ve, ntrl, and +ve faces, respectively.

Conveniently, that cubic and PZ_3 schema can—for any gender—be differentiated into two rhombic schema, the lower rhomb delineating the four 'contracted' *PT*s that have contiguous faces of the same gender (d=0), while the upper rhomb delineates the four 'expanded' *PT*s that have separated faces of that gender (d=1). As in Fig. 10 above, the vertical linkages between corresponding faces of lower d=0 and upper d=1 delineate the *SoF*—for that gender—for each pair of *PT*s for each of the three genders, as the contracted *PT* transforms to the expanded *PT*.

Notwithstanding the remarkable persistence of 3-fold symmetry between the three −ve, ntrl, and +ve genders, critical differences are evident between the neutral, and the −ve and +ve cases. Notably, while the −ve/+ve duality of the cases is realized in the ($\sqrt{2}$) three-dimensional duality of the $OH \leftrightarrow CB$ polar *PP*s ($0_1^- \leftrightarrow \omega_0^- | \alpha_0^+ \leftrightarrow 0_1^+$), and complementarity of the $TO \leftrightarrow TC$ ($\alpha_1^- \leftrightarrow 2_0^- | 2_0^+ \leftrightarrow \omega_1^+$), the corresponding duality in the ntrl cases present two-dimensionally ($\omega_0^0 \leftrightarrow \alpha_0^0$) and ($\omega_1^0 \leftrightarrow \alpha_1^0$), in the duality of faces at level 1 of the rhombic schema. Although the bilateral symmetry and complementarity of the PZ_3 schema dominate the otherwise pervasive 3-fold symmetry of the polyhedral order, the 3-fold symmetry would appear to be more archaic.

Application to core–shell or core–multishell nanomorphologies

As I elsewhere describe in detail [22], the sequences of facial development of the rhombic and PZ_3 schemas can be translated into core–shell (considering one transition), or core–multishell (considering two or all three transitions) morphologies, along the skewed triangular meridionals of the PZ_3 schema. Further, as a consequence of the fundamental harmonic geometry, I propose that these geometries are applicable to developing high purity nanostructured materials—conceivably representing a new class of harmonically engineered materials that might be the antithesis of defect-engineered materials. Source, intermediary, and goal *PT*s are concentric and coaxial. The separation of faces transitions $0_0 \rightarrow 0_1$, $\alpha_0 \rightarrow \alpha_1$ or $\omega_0 \rightarrow \omega_1$, or $2_0 \rightarrow 2_1$ develop as polygonal prisms, the $0_0 \rightarrow 0_1$ transition being a radial, while the neutral $\alpha_0 \rightarrow \alpha_1$ & $\omega_0 \rightarrow \omega_1$ transitions develop as radial rectangles. The $0_0 \rightarrow \alpha_0$ and $0_0 \rightarrow \omega_0$ transitions develop as polygonal pyramids. The $\alpha_0 \rightarrow 2_0$ and $\omega_0 \rightarrow 2_0$ develop as truncated pyramidal frusta (*TPF*s; cupolae) with inner α or ω face and double-frequency outer 2 face, with side walls alternating isosceles triangles and rectangles, the 2*f* neutral case being radial gables (as in $CB \rightarrow SRCO$).

The Polar Zonahedral schema of the Primary Polytopes

The cubic PZ_3 schema, viewed as a progression from source VP to fully formed goal GR, has three major movements or transitions or linkages to the development of the polyhedra within any one class. Initially, the seed VP polytope differentiates in the first transition into the three polar PTs of the +ve, ntrl, and −ve PLs: PL^+, QR, and PL^-. Medially, the three (polar) PTs crossover in the second transition to yield the three (truncated) TPs of the TP^-, SR, and TP^+. Finally, in the third transition, the three truncated TPs integrate to yield the common fruit GR.

The analogous machine learning algorithm for the polar zonagon (2D) or zonahedron (3D) of any natural frequency would separate the input data into primary clusters, mix and match into secondary clusters to compare pairs in sequence, and combine all into the output. This underlying polar zonagonal geometry (together with its polar inversion, the (extended) star) has fascinated traditional Islam as the natural geometry of the center, as evident in its vertical axial extension into the controlling geometry of the polar zonahedral dome as spatial form, its surface decoration, and even as high-rise space truss [10: pp.20–24, Plates B, C] *cf.* 30 St Mary Axe 'The Gherkin' in the City of London.

In the PZ_3 schema, the singular VP, reflecting the initial hierophany, contains the whole polyhedral cosmos in potential, and is characterized by all three contiguous level 0 genders;

- the 3 *initial* transitions of *differentiation* yield the 3 PLs: PL^-, QR, and PL^+, each characterized by one separated strata 0 gender PT, and two contiguous strata 1 gender PTs;
- the 6 *medial* transitions of *crossover* yield the 3 TPs: TP^-, SR, and TP^-, with each characterized by two separated strata 1 gender PTs, and one contiguous level 2 strata PT;
- the 3 *final* transitions of *integration* culminate in the singular goal GR, which is characterized by all three contiguous level 2 genders.

The relevance of the Vesica Pisces rhombic schema of faces

The rhombic schema of faces ($RSoF$; Figs. 4 & 6) has three levels of faces: 0, 1 = α|ω, and 2, while the PZ_3 schema (Figs. 5, 10, 12), has four strata of PPs: 1, 2, 3, and 4. The PZ_3 linkages represent the SoF of one gender for each linkage, in 3 sheaths of −ve, ntrl, and +ve faces, in the core PZ_3 schema view rising left, vertical upward, and rising right, respectively, which sheaths are the zones of the PZ_3. The transitions of the SoFs, which the directed linkages represent, appear to drive the overall transitions of one PT to another, while the steps in rhombic schema level of the other two genders represent the PoFs, usually described as the truncations of the PPs and of their faces. The two PoF transitions of the non-SoF genders exhibit the same behavior, but for the medial transition, differ in level: ($0_1 \rightarrow \alpha_1 | \alpha_0 \rightarrow 2_0$ or $0_1 \rightarrow \omega_1 | \omega_0 \rightarrow 2_0$), with facial type of the middle term polar to the SoF ($\omega_0 \rightrightarrows \omega_1$ or $\alpha_0 \rightrightarrows \alpha_1$), while the initial and final transitions alternate α and ω: $0_0 \rightarrow \alpha_0$ & $0_0 \rightarrow \omega_0$ and $\alpha_1 \rightarrow 2_1$ & $\omega_1 \rightarrow 2_1$, for SoF $0_0 \rightrightarrows 0_1$ and $2_0 \rightrightarrows 2_1$.

For a given gender, faces in a PP are either contiguous, sharing either a VT or a transverse EG, or separated, distanced by a longitudinal EG (from VT of one face to the closest VT of a proximal face), or by another gendered face (from EG to the closest EG).

Thus, the VP of strata 1 has −ve, ntrl, and +ve faces (PTs), each contiguous, all coincident. Strata 2 PTs (PLs) have, by gender, one separated level 0, and two contiguous level 1 (α or ω) faces. Strata 3 PTs (TPs) have, by gender, two separated level 1 (α/ω) faces, and one contiguous level 2 face (sharing a common vertex or edge). Strata 4 PT has 3 separated level 2 faces. Here, the 3D 3*f* symmetry yields to the bilateral complementarity of the 2D projected PZ_3 schema.

The −ve, ntrl, and +ve faces are characterized as: VP: level (0, 0, 0) faces; PL^+, QR, PL^-: (0, α, ω); TP^-, SR, TP^+: (α, ω, 2); GR: (2, 2, 2) (row 3). A measure of the positivity/negativity (+/−vity) of a PP is to multiply the facial levels of the rhombic schema (0, α=ω=1, 2) by the PP's gender (−1|0|+1) (hence the ntrl values become zero, row 4), and sum them (row 5). The complementary $PL^+ \leftrightarrow PL^-$ &

$TP^{+}\leftrightarrow TP^{-}$ are of similar measure $+1 \leftrightarrow -1$, respectively, with $VP{=}QR{=}SR{=}GR{=}0$, and PLs, TPs disposed either side of the $VP{-}QR{\cdots}SR{-}GR$ bilateral plane.

Table I. The generic *PP*s according to their facial level on the rhombic schema & overall gender.

PP	*VP*	*PL*s			*TP*s			*GR*
		PL^{+}	QR	PL^{-}	TP^{-}	SR	TP^{+}	
−|0|+ faces	0 | 0 | 0	0 | ω | α	α | 0 | ω	ω | α | 0	2 | α | ω	ω | 2 | α	α | ω | 2	2 | 2 | 2
face × gender	0 | 0 | 0	0 | 0 | +1	−1 | 0 | +1	−1 | 0 | 0	−2 | 0 | +1	−1 | 0 | +1	−1 | 0 | +2	−2 | 0 | 2
∑ = +/−ity	0	+1	0	−1	−1	0	+1	0

The *PP*s can be further characterized by whether the faces of a gendered axis are contiguous (subscript d=0) or separated (d=1), d being the distance between two proximal faces = edge length:

Table II. The generic *PP*s according to the rhombic schema and their facial separation (d=(0,1)).

PP	*VP*	*PL*s			*TP*s			*GR*
		PL^{+}	QR	PL^{-}	TP^{-}	SR	TP^{+}	
$\text{gender}_{\text{separation}}$	$0_0 \mid 0_0 \mid 0_0$	$0_1 \mid \omega_0 \mid \alpha_0$	$\alpha_0 \mid 0_1 \mid \omega_0$	$\omega_0 \mid \alpha_0 \mid 0_1$	$2_0 \mid \alpha_1 \mid \omega_1$	$\omega_1 \mid 2_0 \mid \alpha_1$	$\alpha_1 \mid \omega_1 \mid 2_0$	$2_1 \mid 2_1 \mid 2_1$

If parity is defined as the sum of the level on the rhombic schema (0, 1, or 2) and the distance apart of faces of d (0 or 1), this is conserved, so at strata 1 of the *STM*s of the PZ_3 cubic schema, parity for each of the 3 gendered faces is 0; at strata 2, 1; at strata 3, 2; and at strata 4, 3; *in toto* (0, 3, 6, 9) per *PP*.

The *VP* is characterized as all three gendered sets of contiguous faces; the *PL*s by one gendered set of level 0 separated faces and two gendered sets of one or two level 1 contiguous faces; the *TP*s by two gendered sets of one or two level 1 separated faces and one gendered set of level 2 contiguous faces; and the *GR* by all three gendered sets of separated faces.

The generic *PP*s can similarly be described by their number and gender of separation of faces, so numerically, the *VP* has undergone 0 *SoF*s, the *PL*s have 1, the *TP*s 2, and the *GR* 3:

Table III. The generic *PP*s according to their separation of faces and by gender.

PP	*VP*	*PL*s			*TP*s			*GR*
		PL^{+}	QR	PL^{-}	TP^{-}	SR	TP^{+}	
No. of *SoF*s	0 | 0 | 0	1 | 0 | 0	0 | 1 | 0	0 | 0 | 1	0 | 1 | 1	1 | 0 | 1	1 | 1 | 0	1 | 1 | 1

In terms of gender, *VP* has undergone no *SoF*; each *PL* has undergone 1 *SoF* of its gender; each *TP* has 2 *SoF*s, but not of its gender; while *GR* has 3 *SoF*s, 1 of each of the 3 genders.

Nomenclature: *, 'colored' • Class I 3D: OH^{*} = tetra-tetrahedron ($TR{:}TR$); $CO^{*} = SR\ TR{:}TR$; $TO^{*} = GR\ TR{:}TR$ • Class II 3D: *OH*, octahedron; *CO*, cuboctahedron; *CB*, cube; *TO*, truncated octahedron; *SRCO*, small rhombic cuboctahedron; *TC*, truncated cube; *GRCO*, great rhombic cuboctahedron • Class III 2D: *DG*, decagon; *PN*, pentagon; *RP*, rotated pentagon ○ Class III 3D: *DC*, dodecahedron; *GRID*, great rhombic icosidodecahedron; *IC*, icosahedron; *ID*, icosidodecahedron; *SRID*, small rhombic icosidodecahedron; *TD*, truncated (trunc.) dodecahedron; *TI*, trunc. icosahedron • Class IV 2D: Component arrays: vt, verticial; tr, triangular; hx, hexagonal; rt, rotated triangular; rx, rotated hexagonal; $2t$, 2f triangular (hexagonal); $2x$, 2f hexagonal (dodecagonal) ○ Combined arrays (+ve:−ve): $vt{:}\,vt$, verticial:verticial; $tr{:}\,vt$, triangular:verticial; $vt{:}\,hx$, verticial:hexagonal; $rt{:}\,rx$, rotated triangular:rotated hexagonal; $2t{:}\,rx$, hexagonal (2f triangular):rotated hexagonal; $rt{:}\,2x$, rotated triangular:2f hexagonal (dodecagonal); $tr{:}\,hx = SR\ tr{:}\,hx$, triangular:hexagonal; $2t{:}\,2x$, 2f triangular:2f hexagonal (dodecagonal) • Class V 2D Component arrays: vt, verticial; sq, square; ns, neutral square; rs, rotated square; $2s$, 2f square (octagonal) • Combined arrays (+ve:−ve): $vt{:}\,vt$, verticial:verticial; $sq{:}\,vt$, square:verticial; $vt{:}\,sq$, verticial:square; $rs{:}\,rs$, rotated square:rotated (trunc.) square; $2s{:}\,rs$, octagonal (2f square):rotated square; $rs{:}\,2s$, rotated square:2f square (octagonal); $sq{:}\,sq = SR\ sq{:}\,sq$, square:square; $2s{:}\,2s = GR\ sq{:}\,sq$, 2f square:2f square = $OG{:}\,OG$ • Generic: −ve, negative; ntrl, neutral; +ve, positive; *V*, *VT*, vertex; *VP*, verticial polytope; *NV*, neutral vertex; *EG*, edge; *NE*, neutral edge; *F*, face; *FT*, facial polytope; *PG*, polygon; *PT*, polytope; *NS*, neutral square; *PoF*, Progression of Faces; *PRS*, prism; *PYR*, pyramid; *RSoF*, rhombic schema of faces; *SoF*, separation of faces ○ 'rotated' faces are truncated faces (duals) ■

The facial development by gender accompanying the separation of faces

The regularity of the transitions accompanying the separation of faces between two linked *PP*s in the PZ_3 schema then also becomes apparent:

Table IV. The generic progression of facial development by −ve, ntrl, and +ve gender according to the PZ_3 and rhombic schema according to the *SoF*, centered on the *VP–QR–GR* axis.

IV.	Generic progression of facial development by gender according to the PZ_3 schema of the *SoF*.																	
Goal PT	GR [GR CO]																	
Gender	−ve	ntrl	+ve	−ve		ntrl		+ve		−ve		ntrl		+ve		−ve	ntrl	+ve
Final Integral Meridional Transition	2_1 ↑ ω_1	2_1 ⇑ 2_0	2_1 ↑ α_1	2_1 ↑ α_1		2_1 ↑ ω_1		2_1 ⇑ 2_0		2_1 ⇑ 2_0		2_1 ↑ α_1		2_1 ↑ ω_1		2_1 ↑ ω_1	2_1 ⇑ 2_0	2_1 ↑ α_1
Source/ Goal PT	↺	SR	[SR CO]	↻		TP^+ [TO]		↺		↻		TP^- [TC]		↺		↻	SR	[SR CO]
Gender	−ve	ntrl	+ve	−ve	ntrl	+ve	−ve	ntrl	+ve	−ve	ntrl	+ve	−ve	ntrl	+ve	−ve	ntrl	+ve
Medial Crossover Skwd Eqtrl Transition	ω_1 ↑ 0_1	2_0 ↑ ω_0	α_1 ⇑ α_0	α_1 ↑ 0_1	ω_1 ⇑ ω_0	2_0 ↑ α_0	α_1 ⇑ α_0	ω_1 ↑ 0_1	2_0 ↑ ω_0	2_0 ↑ α_0	α_1 ↑ 0_1	ω_1 ⇑ ω_0	2_0 ↑ ω_0	α_1 ⇑ α_0	ω_1 ↑ 0_1	ω_1 ⇑ ω_0	2_0 ↑ α_0	α_1 ↑ 0_1
Source/ Goal PT	PL^+ [OH]			QR [CO]			PL^- [CB]											
Gender	−ve	ntrl	+ve	−ve	ntrl	+ve	−ve	ntrl	+ve									
Initial Differential Meridional Transition	0_1 ⇑ 0_0	ω_0 ↑ 0_0	α_0 ↑ 0_0	α_0 ↑ 0_0	0_1 ⇑ 0_0	ω_0 ↑ 0_0	ω_0 ↑ 0_0	α_0 ↑ 0_0	0_1 ⇑ 0_0									
Source PT	VP [VP]																	

−ve, negative; ntrl, neutral; +ve, positive. Skwd Eqtl, Skewed Equatorial; ⇑, Separation of Faces (*SoF*) of one gendered face; ↑, accompanying Progression of Faces (*PoF*; transition of level) of the other two gendered faces. Subscripts differentiate the contiguous d=0 and separated d=1 cases. Of the 3 horizontal bands of information, the bottom band describes the initial differentiation of the strata 1 seed *VP* into the 3 strata 2 polar *PT*s; middle band describes the medial crossover transitions of the strata 2 *PT*s to strata 3 truncated polar *PT*s following the transitions of the PZ_3 schema along the alternating clockwise and counterclockwise, skewed triagonal meridionals of the PZ_3 schema (there is no differentiation of priority between the width of the transitional cells; they are equivalent); top band describes the final integration of the three strata 3 *PT*s to culminate in the strata 4 *GR*. For each transition, the two *PT*s at right in square parentheses refer to the two corresponding Class II *PP*s of that transition: source and goal.

In this analysis, switching $\alpha \leftrightarrow \omega$ for the −ve, and for the ntrl, allows the 3-fold symmetry of the PZ_3 schema by gender to be revealed, treating ntrl as in many senses an equivalent gender to −ve and +ve, rather than qualitatively different. The new convention varies facial type by axis (except for the *VP* & *GR*), while better reflecting the duality inherent in the bilateral nature of the PZ_3 schema, offering superior imageability for further research and application.

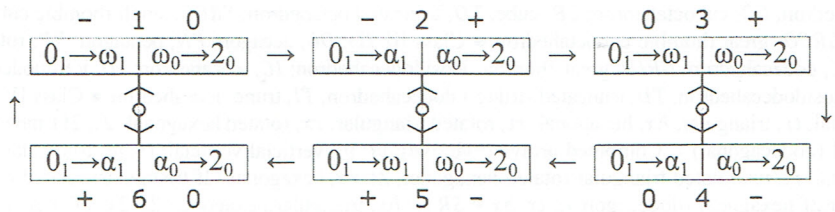

Figure 11: Class II cyclic *PoF* complementarity of the facial progressions of the two non-*SoF* genders.

The *SoF* phenomenon according to the PZ_3 schema, and the *PoF* according to the rhombic schema, appear complementary, while within the *PoF*, the initial differential and final integral transitions are complementary, as also are the *PoF*s in Fig. 11 above, abstracted from Table IV.

Table V. Generic Skewed triagonal meridionals of the unfurled 3-frequency Polar Zonahedral (PZ_3) schema of the Primary Polytopes about the $VP\cdots SR–GR$ axis, with exemplar Class II figures.

V.	Generic Skewed triagonal meridionals of the PZ_3 schema of the Primary Polytopes, and for Class II.																	
Medial *PT* sequence	**QR→TP⁻**			**TP⁻←PL⁻**			**PL⁻→SR**			**SR←PL⁺**			**PL⁺→TP⁺**			**TP⁺← QR**		
Generic seq.	VP→QR→TP⁻→GR			GR←TP⁻←PL⁻←VP			VP→PL⁻→SR→GR			GR←SR←PL⁺←VP			VP→PL⁺→TP⁺→GR			GR←TP⁺←QR←VP		
Class II seq.	VP→CO→TC→GRCO			GRCO←TC←CB←VP			VP→CB→SRCO→GRCO			GRCO←SRCO←OH←VP			VP→OH→TO→GRCO			GRCO←TO←CO←VP		
Exemplar figure for Class II {2,3,4} symmetry	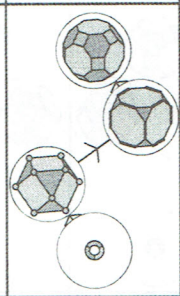			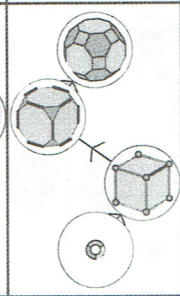			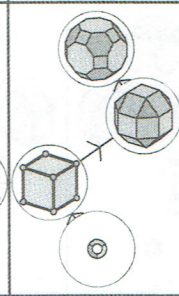			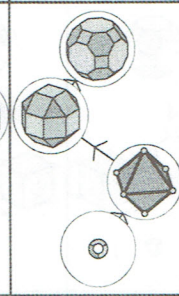			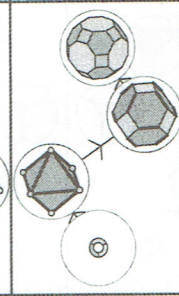			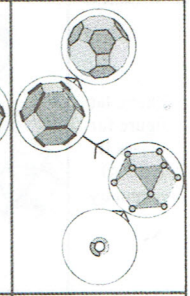		
#	1↻			2↺			3↻			4↺			5↻			6↺		
Face gender	−ve	ntrl	+ve	−ve	ntrl	+ve	−ve	ntrl	+ve	−ve	ntrl	+ve	−ve	ntrl	+ve	−ve	ntrl	+ve
GR	GR			GR			GR			GR			GR			GR		
Final Integral Meridional Transition	2_1 ⇑ 2_0	2_1 ↑ α_1	2_1 ↑ ω_1	2_1 ⇑ 2_0	2_1 ↑ α_1	2_1 ↑ ω_1	2_1 ↑ ω_1	2_1 ⇑ 2_0	2_1 ↑ α_1	2_1 ↑ ω_1	2_1 ⇑ 2_0	2_1 ↑ α_1	2_1 ↑ α_1	2_1 ↑ ω_1	2_1 ⇑ 2_0	2_1 ↑ α_1	2_1 ↑ ω_1	2_1 ⇑ 2_0
TP	TP⁻			TP⁻			SR			SR			TP⁺			TP⁺		
Medial Crossover Skewed Equatorial Transition	2_0 ↑ α_0	α_1 ↑ 0_1	ω_1 ⇑ ω_0	2_0 ↑ ω_0	α_1 ⇑ α_0	ω_1 ↑ 0_1	ω_1 ⇑ ω_0	2_0 ↑ α_0	α_1 ↑ 0_1	ω_1 ↑ 0_1	2_0 ↑ ω_0	α_1 ⇑ α_0	α_1 ↑ 0_1	ω_1 ⇑ ω_0	2_0 ↑ α_0	α_1 ⇑ α_0	ω_1 ↑ 0_1	2_0 ↑ ω_0
PL	QR			PL⁻			PL⁻			PL⁺			PL⁺			QR		
Initial Differential Meridional Transition	α_0 ↑ 0_0	0_1 ⇑ 0_0	ω_0 ↑ 0_0	ω_0 ↑ 0_0	α_0 ↑ 0_0	0_1 ⇑ 0_0	ω_0 ↑ 0_0	α_0 ↑ 0_0	0_1 ⇑ 0_0	0_1 ⇑ 0_0	ω_0 ↑ 0_0	α_0 ↑ 0_0	0_1 ⇑ 0_0	ω_0 ↑ 0_0	α_0 ↑ 0_0	α_0 ↑ 0_0	0_1 ⇑ 0_0	ω_0 ↑ 0_0
VP	VP			VP			VP			VP			VP			VP		

seq., sequence; −ve, negative; ntrl, neutral; +ve, positive; Skwd. Eqtrl., Skewed Equatorial. ⇑, Separation of faces of one gendered face; ↑, accompanying progression of faces (transition of level) of the other two genders. Subscripts differentiate the contiguous d=0 and separated d=1 cases. Of the 4 horizontal bands of information, the lowest band describes the initial differentiation of the strata 1 seed *VP* into the 3 strata 2 polar *PT*s; the two middle bands describe the medial crossover transitions of the strata 2 PTs to strata 3 truncated polar *PT*s following the transitions of the PZ_3 schema along the (lower band) clockwise, and (upper band) counterclockwise, *STM*s of the PZ_3 schema; while the uppermost band describes the final integration of the three strata 2 *PT*s to culminate in the strata 4 *GR*.

The skewed triagonal meridionals of the development of *PT*s by the separation of faces

Recent work on chiral molecular polyhedra demonstrates the importance of facial interactions and separation in complex assemblies [23]. As previously presented [21, 22], but here refined, with critically redefined α↔ω dialectic convention that replaces the earlier α↔β dialectic convention, the (rotated cubic) PZ_3 schema of the polyhedra based on the separation of faces can be understood as 6 progressions along the skewed triangular meridionals (*STM*s) of the cube, 3 clockwise and 3 counter-clockwise on the PZ_3 schema. Each *STM* consists of 3 linked edges of the schematic cube, developing through the 4 strata in the generic order $VP\rightarrow PL\rightarrow TP\rightarrow GR$. The 6 *STM*s are shown left to right as an unfurling about the vertical axis through the $VP–SR–GR$ meridian of the PZ_3 schema from a vertical fissure through the $VP–QR–GR$ meridion, viewed from without, not within.

Table VI. Overlay of the *PoF* by axis of the Class II Skewed triagonal meridionals of the unfurled PZ_3 schema about the $VP\cdots SR{-}GR$ axis, and generic *SoF* and *PoF* transitions of faces.

VI.	Overlay of the progression of faces by axis of the PZ_3 schema Skewed triagonal meridionals of Class II.					
Medial PT sequence	QR→TP⁻	TP⁻←PL⁻	PL⁻→SR	SR←PL⁺	PL⁺→TP⁺	TP⁺← QR
Generic seq.	VP→QR→TP⁻→GR	GR←TP⁻←PL⁻←VP	VP→PL⁻→SR→GR	GR←SR←PL⁺←VP	VP→PL⁺→TP⁺→GR	GR←TP⁺←QR←VP
Class II seq.	VP→CO→TC→GRCO	GRCO←TC←CB←VP	VP→CB→SRCO→GRCO	GRCO←SRCO←OH←VP	VP→OH→TO→GRCO	GRCO←TO←CO←VP
Exemplar figure for Class II {2,3,4} symmetry	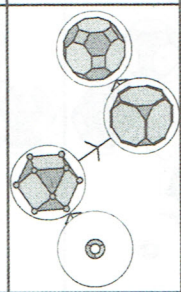	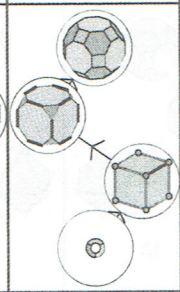	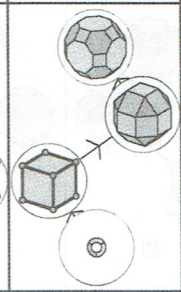	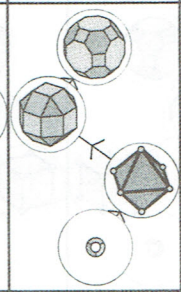	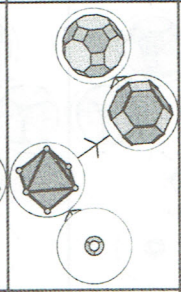	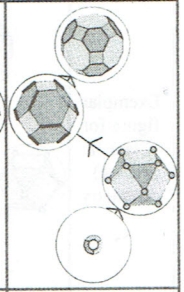
#	1↻	2↺	3↻	4↺	5↻	6↺
Negative	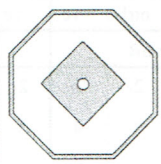	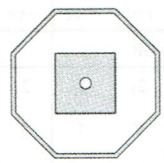	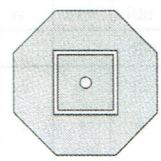	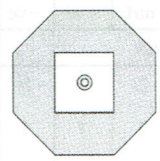	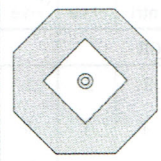	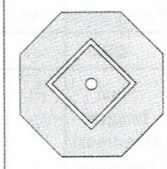
Neutral	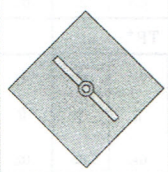	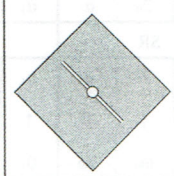	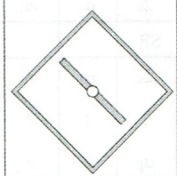	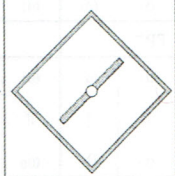	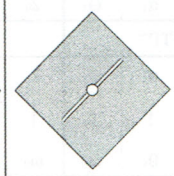	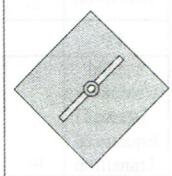
Positive	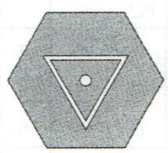	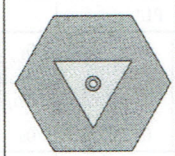	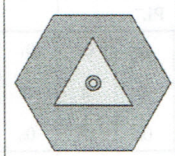	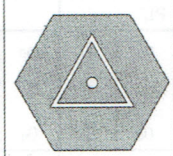	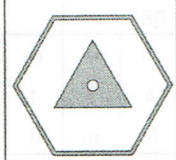	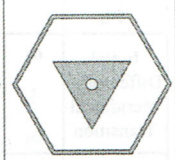
Negative	$0_0 \rightarrow \alpha_0 \rightarrow 2_0 \rightrightarrows 2_1$	$2_1 \rightrightarrows 2_0 \leftarrow \omega_0 \leftarrow 0_0$	$0_0 \rightarrow \omega_0 \rightrightarrows \omega_1 \rightarrow 2_1$	$2_1 \leftarrow \omega_1 \leftarrow 0_1 \rightrightarrows 0_0$	$0_0 \rightrightarrows 0_1 \rightarrow \alpha_1 \rightarrow 2_1$	$2_1 \leftarrow \alpha_1 \rightrightarrows \alpha_0 \leftarrow 0_0$
Neutral	$0_0 \rightrightarrows 0_1 \rightarrow \alpha_1 \rightarrow 2_1$	$2_1 \leftarrow \alpha_1 \rightrightarrows \alpha_0 \leftarrow 0_0$	$0_0 \rightarrow \alpha_0 \rightarrow 2_0 \rightrightarrows 2_1$	$2_1 \rightrightarrows 2_0 \leftarrow \omega_0 \leftarrow 0_0$	$0_0 \rightarrow \omega_0 \rightrightarrows \omega_1 \rightarrow 2_1$	$2_1 \leftarrow \omega_1 \leftarrow 0_1 \rightrightarrows 0_0$
Positive	$0_0 \rightarrow \omega_0 \rightrightarrows \omega_1 \rightarrow 2_1$	$2_1 \leftarrow \omega_1 \leftarrow 0_1 \rightrightarrows 0_0$	$0_0 \rightrightarrows 0_1 \rightarrow \alpha_1 \rightarrow 2_1$	$2_1 \leftarrow \alpha_1 \rightrightarrows \alpha_0 \leftarrow 0_0$	$0_0 \rightarrow \alpha_0 \rightarrow 2_0 \rightrightarrows 2_1$	$2_1 \rightrightarrows 2_0 \leftarrow \omega_0 \leftarrow 0_0$

Vertices shown as small circles; neutral α and ω faces (edges) shown as 2-gons; separation of faces: ⇉ (−ve *VT*, *SQ*, *RS*, & *OG*; ntrl *VT*, *EG*, & *SQ*; +ve *VT*, *TR*, *RT*, & *HX*) shown as double-line polygons. Each gendered axial face progresses 0→α→2 or 0→ω→2, punctuated by one *SoF*. Subscripts in the last three rows refer to the generic spacing of faces from the *SoF* of d=0 ⇉ 1 (contiguous ⇉ separated), the *PoF* of the other two genders always conserving d.

Table VI above shows these progressions of faces of a particular gender on its symmetry axis. For Class II as exemplar, stylized axial views of each of the Skewed Triagonal Meridional (*STM*) progressions of faces on the −ve, ntrl, and +ve axes are shown. In each transition *PP* to *PP*, there is a *SoF* on each of the gendered axes; for any *STM*, there are 3 *SoF*s, one −ve, one ntrl, & one +ve: one strata 1 ⇉ 2, one strata 2 ⇉ 3, and one strata 3 ⇉ 4 (initial, medial, & final).

The first of the three transitions of *PP*s of each *STM* is meridional; the second is skewed equatorial, being either clockwise or counterclockwise; while the third is again meridional. The faces of each *PP* may be considered to progress along each of the *STM*s, and to do so regularly according to the cyclic harmony evident in the table. For each gender, the facial types of those axes always progress in the

rhombic schema sequence $0\rightarrow\alpha\rightarrow2$ or $0\rightarrow\omega\rightarrow2$, punctuated by one *SoF* at the initial, medial, or final stage. For each transition of *PP*s, one gendered facial transition is the separation of faces, so conserves the level of *PT* on the rhombic schema while transitioning from contiguous (d=0) to separated (d=1), so either −ve-, ntrl-, or +ve-gendered $0_0\rightrightarrows0_1$, $\alpha_0\rightrightarrows\alpha_1$ or $\omega_0\rightrightarrows\omega_1$, or $2_0\rightrightarrows2_1$. The other two gendered (non-*SoF*) faces for that transition of *PT* progress one level on the rhombic schema (a *PoF*), while conserving their contiguous or separated status (d). In that development, for each *STM*, in the first, meridional transition, one face progresses $0_0\rightarrow\alpha_0$ and one face progresses $0_0\rightarrow\omega_0$ while conserving d=0, while one face separates ($0_0\rightarrow\alpha_0$, $0_0\rightarrow\omega_0$, and $0_0\rightrightarrows0_1$). In the second, skewed equatorial transition, the face that has separated progresses while conserving d=1, i.e., $0_1\rightarrow(\alpha_1$ or $\omega_1)$; one of the other two faces progresses while conserving d=0, i.e., $(\alpha_0$ or $\omega_0)\rightarrow2_0$ of the same rhombic schema pole (α or ω), while the other rhombic schema pole (ω or α) separates $\omega_0\rightrightarrows\omega_1$ or $\alpha_0\rightrightarrows\alpha_1$, so either: ($0_1\rightarrow\alpha_1$, $\alpha_0\rightarrow2_0$, $\omega_0\rightrightarrows\omega_1$) or: ($0_1\rightarrow\omega_1$, $\omega_0\rightarrow2_0$, $\alpha_0\rightrightarrows\alpha_1$). In the third, meridional transition, the face that has just separated progresses $\alpha_1\rightarrow2_1$ or $\omega_1\rightarrow2_1$; the face (of the other rhombic schema pole) that had initially separated progresses $\omega_1\rightarrow2_1$ or $\alpha_1\rightarrow2_1$, while the remaining face separates $2_0\rightrightarrows2_1$, so either: ($\alpha_1\rightarrow2_1$, $\omega_1\rightarrow2_1$, $2_0\rightrightarrows2_1$) or: ($\omega_1\rightarrow2_1$, $\alpha_1\rightarrow2_1$, $2_0\rightrightarrows2_1$).

The return to duality

The *SoF* uniquely determines the objective (cubic) PZ_3 form; but while the pairs PL^+–TP^+ are linked (left), as are PL^-–TP^- (right), *QR* and *SR* are not, but are polar; hence the 3-fold symmetry of the order yields to bilateral complementarity about the ntrl *VP*–*QR*···*SR*–*GR* plane (the central 'vertical' axis in Fig. 12 below, and seen in Fig. 13 from above (top), and below).

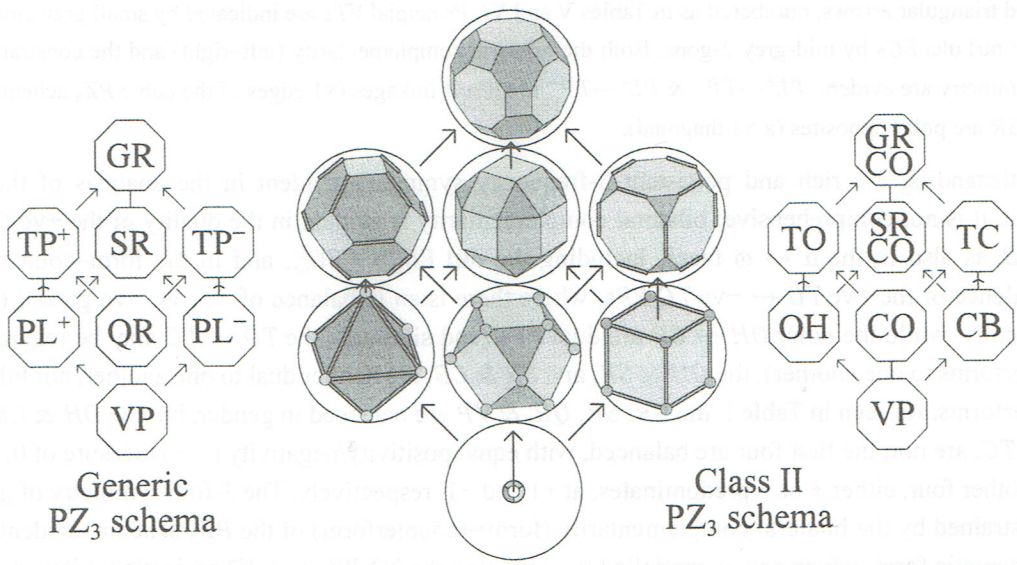

Figure 12: The 2.5D Generic (left) and Class II (center & right) PZ_3 schema of bilateral complementarity that provides above–below, front–back, & left–right existential differentiation.

Thus, each *PP* is involved in three *SoF*s. The Strata 1 *VP* generates three *SoF*s, one per gender. The three Strata 2 *PP*s (PL^-, *QR*, PL^+) each inherit one *SoF*, and generate two *SoF*s in the other two genders. The three Strata 3 *PP*s (TP^-, *SR*, TP^+) each inherit two *SoF*s, and generate one *SoF* in the remaining gender. The Strata 4 *GP* inherits three *SoF*s, one per gender.

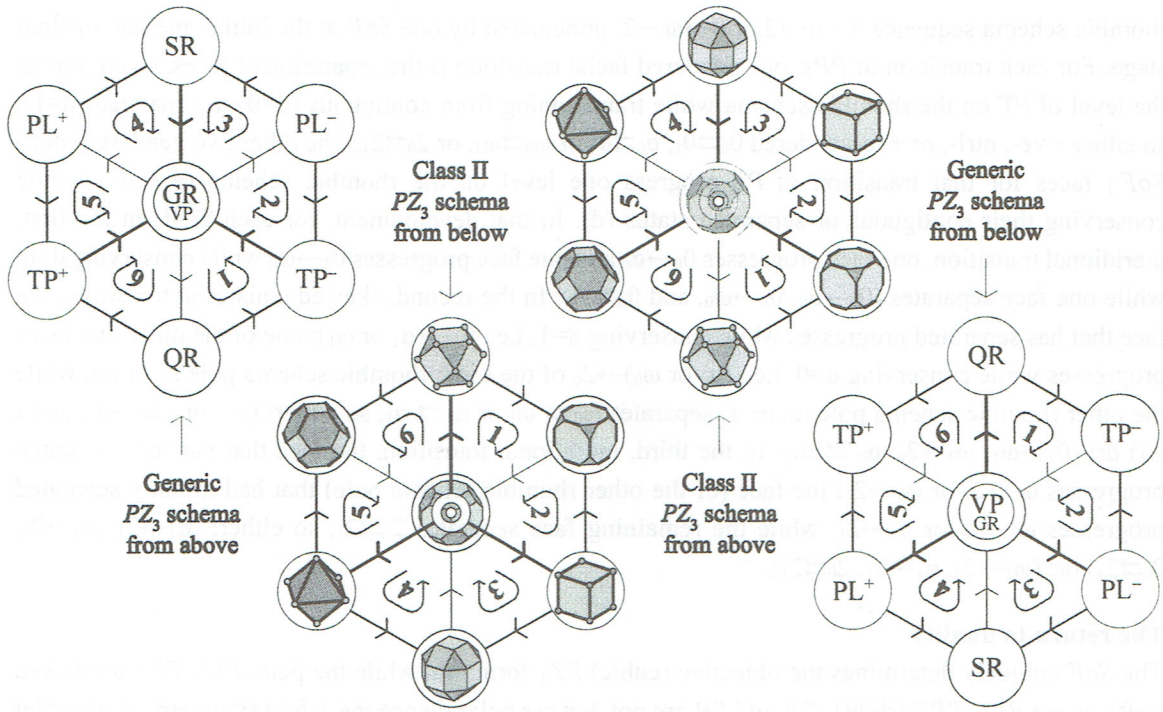

Figure 13: Generic (black & white) and Class II (grey) PZ_3 schema on the main *VP—GR* axis from above (top)**, and below** (bottom)**.** Arrowed links indicate the *SoF* transitions $PP \rightarrow PP$; *STM* progressions indicated by rounded triangular arrows, numbered as in Tables V and VI. Principial *VT*s are indicated by small grey circles by gender; ntrl α|ω *EG*s by mid-grey 2-gons. Both the bilateral complementarity (left–right) and the constrained 3-fold symmetry are evident: $PL^+ \rightarrow TP^+$ & $PL^- \rightarrow TP^-$ are direct linkages (√1 edges of the cubic PZ_3 schema), but *QR* & *SR* are polar opposites (a √3 diagonal).

Notwithstanding the rich and persistent 3-frequency symmetry evident in the analysis of the PZ_3 schema, it is not comprehensive; bilateral complementarity is evident in the duality of the +ve $OH \leftrightarrow$ −ve CB, as also in the α ↔ ω faces, including the ntrl $EG^0_\alpha \leftrightarrow EG^0_\omega$, and in the form–counterform equivalence of the +ve $TO \leftrightarrow$ −ve TC *PP*s, where there is an imbalance of +ve *vs.* −ve gender (Table I). Patently, while the polar $OH \leftrightarrow CB$ are dual *PP*s (and similarly, the $TO \leftrightarrow TC$ may be regarded as counterforms to one another), the OH & SR, and SR & CB, are neither dual to one another, nor bilateral counterforms. As seen in Table I, the GR, SR, QR, & VP are balanced in gender, but the OH & CB, and TO & TC, are not; the first four are balanced, with equal positivity/negativity (+/−) measure of 0, while in the other four, either + or − predominates, at +1 and −1, respectively. The 3-fold symmetry of gender is constrained by the bilateral complementarity (form↔counterform) of the PZ_3 schema, evident in its 2D schematic form, which can be modelled by flattening the 3D PZ_3 to a 2D projection, viewed with a central vertical axis that runs from the GR to the SR and the QR to the VP, the SR and QR unlinked, with the +ve PL^+ & TP^+ to one side (the left in my model from without; the right from within), and the −ve PL^- & TP^- to the other (the right from without). In class II, the central vertical axis is $GRCO$-$-SRCO\cdots CO-VP$, the $SRCO$ and CO unlinked, with the +ve OH and TO to one side, and the −ve CB and TC to the other; the QR (CO) (otherwise split in two at the left & right of the unfurled schema in Tables 5 & 6) remains at the center. The 3D 3*f* symmetry yields to 2D bilateral complementarity, whether at the level of form ↔ counterform ($TO \leftrightarrow TC$), or pure duality (of 3D $OH \leftrightarrow CB$, and 2D facial α↔ω for the *PP*s in general). Both symmetries persist in a creative tension as the PZ_3 schema is alternately visualized in its 3D and 2D forms. In my next paper in this series, I anticipate looking in more depth at this notion of bilateral complementarity that characterizes the order of the polyhedra.

Conclusion

This paper further develops a highly imageable model to account for the development of form in the regular and semi-regular 2D and 3D polytopes, generically across all five classes, and exemplary for Class II of {2,3,4} symmetry. This order is based on the distinction of principial faces from pragmatic, which principial faces allow 1-gon *VT*s or 2-gon *EG*s of zero extent or width, and the recognition of a seminal verticial *PT* in each class. These enable the development of the *PoF* rhombic schema and of the 3-frequency *PZ* schema abstracted from the *SoF*: in each class, for each gender, each face occurs twice; first in the contracted contiguous form, where pairs of proximal faces share a common *VT* or *EG*. In the *SoF*, they expand into separated form, separated by an edge or face of different gender along their axis of separation, and correspond to the lower and higher rhomb, respectively, of the PZ_3 schema.

This order appears rigorous, and generates insights into the morphology of these 2D and 3D *PT*s, both generically, and exemplary for Class II. The PZ_3 schema suggests an ordered development of the *PP*s within any one class, from *VP* to *GR*, which appears to be driven by the *SoF* phenomenon, together with the associated two *PoF*s by gender according to the *RSoF*. The order of *PP*s appears to be characterized by a primordial 3*f* symmetry that develops a tripartite gendered structure organized about a unique main *VP*–*GR* axis, that is then constrained into bilateral complementarity about the *VP*–*QR*···*SR*–*GR* vertical plane, which complementarity includes duality, also axially as √3 polar pairs.

Creative tension is apparent between the two organizing principles of 3-fold symmetry about the vertical main axis, and complementarity about the main bilateral plane, which is reflected in the ambiguity of the 2.5D PZ_3 schema, which in its 3D form unveils the 3-fold symmetry, while in its 2D form, emphasizing the bilateral complementarity. The 3-fold archaic nature appears ephemeral and transcendent; the 2-fold complementarity pragmatic and existential. To considerable degree, the ntrl gender acts equivalently to the +ve and −ve genders, so the three genders can almost be considered as equal players in a tripartite system, as reflected in the three-fold symmetry of the prototypical PZ_3 schema. Yet the ntrl gender develops a form—counterform complementarity *viz-à-vis* the +ve and −ve genders; the +ve and −ve genders develop an external form—counterform complementarity to one another, while the ntrl develops an internal self-complementarity at the levels of *PP*s ($PL^+ \leftrightarrow PL^-$ duality and $TP^+ \leftrightarrow TP^-$ complementarity), and faces (α↔ω facial form–counterform ability).

In the evolution of form, gender arises in a two-step process. First, the distinction between ntrl and polar arises; second, both cases differentiate – the polar *externally* into a +ve ↔ −ve dialectic of primary *PT*s, the ntrl *internally* into an α↔ω dialectic of ntrl faces, the two dialectics mirroring one another.

I have traced the evolution of form in the cubic schema, considered as a 3-frequency polar zonahedron (PZ_3), disposed on a vertical √3 axis from base *VP* to polar opposite crowning *GR*. This disposition and orientation of the cubic schema with a unique vertical major *VP*—*GR* axis differentiates the 8 *PT*s of any one of the five symmetry classes into 4 strata and subclasses of *PT*s: the seed *VP*, from which the class of *PT*s springs; the lower polar band of PL^-, *QR*, & PL^+ that the *VP* first gives rise to; the higher truncated polar band of TP^+, *SR*, & TP^- that the second band elements connect to, and the crowning *GR* that the third band elements return to.

The 'vertical' progression in the PZ_3 schema might thus be considered to have four vertically differentiated strata of *PT*s, with three zones of transformation between them. The first polar zone is the initializing *three-fold separation* from the base *VP* to the lower band of PL^-, *QR*, & PL^+. The second equatorial zone is characterized by each of the three latter *PT*s *bifurcating to recombine in pairs* to link to the higher band of TP^+, *SR*, & TP^-. The third polar zone is then the finalizing *three-fold reunion* of those three elements to culminate in the crowning *GR*.

The *PT*s in any of 5 symmetry classes can thus be systematically differentiated into the four subclasses *VP* | PL^-, *QR*, & PL^+ | TP^+, *SR*, & TP^- | *GR*, which qualitatively differ. They can then be

further differentiated by three-fold gender of −ve (PL^- & TP^-), ntrl (VP, QR, SR, & GR), and +ve (PL^+ & TP^+). The ntrl can be classified into major (VP & GR) and minor (QR & SR) ntrls; in elevation (Fig. 12) and plan view (Fig. 13), the PZ_3 schema reminds that only GR and VP are truly axial; in contrast, QR and SR, like $PL^{+/-}$ and $TP^{+/-}$, lie on the skewed equatorial band, again emphasizing their 'lower' tripartite polar nature, rather than the true 'higher' neutrality of the VP and GR. In that sense, neutrality takes two forms and presents at two levels—firstly of the comprehensive overarching absolute (VP and GR), and secondly of the relative (QR and SR) as one of the three tripartite genders.

Consideration of the pervasive 3-fold order of the PZ_3 schema suggests there is merit in considering the QR to function in part as the Polar Neutral PL^0, and the SR as the Truncated Polar Neutral TP^0; these redefinitions suggest considering VP and GR as elements of that order that represent all 3 genders simultaneously in an overall −ve|ntrl|+ve tripartite system. This emphasizes the horizontal consistency of the constituent elements within a layer, as well as their consistent differentiation by polar quality, in terms of tripartite gender and associated vertical consistency. That exploration of the cluster of ideas is insightful, and to some extent better characterizes the nature of the order; the regular disposition of PPs in the PZ_3 schema and the consistency of their interrelationships strongly suggests the archaic quality of the 3-fold symmetrical nature of their order. But the above↔below, front↔back, and left↔right existential form–counterform bilateral complementarity remains undeniable, and restores the usual sense of neutrality to the VP, QR, SR, GR, and to the level 0 & 2 faces, and the sense of bipolar +ve/−ve relationship of the $PL^+ \leftrightarrow PL^-$ duality and $TP^+ \leftrightarrow TP^-$, the polar pairs $VP \leftrightarrow GR$, $PL^- \leftrightarrow TP^+$, $QR \leftrightarrow SR$, and $PL^+ \leftrightarrow TP^-$ (yet to be addressed), and the α↔ω facial, form–counterform dual relationships.

This should give the reader a better sense of the qualification of the PTs within any symmetry class, and the rigorous consistency of the formal interrelationships across all five classes. The relationships of the exemplar Class II are generic, applying to all three Classes I–III of the polyhedra, and Classes IV & V of the tessellations, allowing for their nature of 3D finite form *vs.* 2D infinite array. The individual PTs within a class are not of mundane equivalence, but highly differentiated expressions of an integral order. That order appears to be characterized by an archaic 3D 3-fold symmetry, constrained by a fundamental 2D bilateral complementarity of form–counterform that can be projected from the 3D PZ_3 schema to its 2D state. In a developmental sense, the 3-fold symmetry logically predates the subsequent imposition of bilateral form in the emergence of these forms from an initial hierophany that more clearly reflects their noumenal nature, to realization in the phenomenal world. This perspective better suits a traditional symbolic, sacred geometrical, or morphological approach, than a profane perspective that finds both kinds of symmetry to coexist as different facets of the same atemporal order. Such a developmental sense extends earlier work, which found profound human meaning in the development implicit in the polar zonagon (as polar inversion of the regular star), with geometric cosmogeny of creation → manifestation → reunion. It is no coincidence that the natural geometry of the center (the counterform of the star) it unveils has preoccupied traditional Islamic architecture [10].

Future work would refine my previously advanced order of the all-space-filling polyhedra and tessellations (honeycombs) in the light of these more recent explorations, addressing the complementarity by gender and by level of development from contiguous to separated PTs.

This paper addresses the need for an accessible, facile, coherent, and imageable order of the regular and semi-regular polyhedra and tessellations for applications that are becoming increasingly germane, such as microgravity applications, whether through scale (materials characterizations, nanomaterial morphology), or deployment in Space (habitations and large-scale structures, manufacturing, spatial organization), and more profoundly, the reemergence of a meaningful symbolism (Sacred geometry/art/architecture/ aesthetics) that, in my opinion, the current environmental crisis—and its root cause, the underlying spiritual crisis of the modern world—direly needs.

References

[1] K. Critchlow, Order in Space. Thames and Hudson, London, 1969.

[2] B. Grünbaum and G. C. Shephard, Tilings and Patterns. W. H. Freeman, New York, 1987.

[3] M. Conforti, L. Wolsey, Facet separation with one linear program, Mathematical Programming, 2019.

[4] S. E. Wright, On the Dimension of a Face Exposed by Proper Separation of Convex Polyhedra, Discrete & Computational Geometry, 2010.

[5] Y. Gérard, About the Decidability of Polyhedral Separability in the Lattice Zd - Recognizing Digital Polyhedra with a Prescribed Number of Faces, J. Math. Imaging Vis., 2017.

[6] V. I. Subbotin, On Polyhedra with Rhombic Vertices and Regular Faces, Journal of Mathematical Sciences, 2023.

[7] X. Allamigeon, R. D. Katz, P.-Y. Strub, Formalizing the Face Lattice of Polyhedra, Automated Reasoning, 2020.

[8] B. Grünbaum, Parallelogram-faced isohedra with edges in mirror-planes, Discret. Math., 2000.

[9] S. Hyde, M. E. Evans, Symmetric tangled Platonic polyhedra, Proceedings of the National Academy of Sciences, 2022

[10] R. C. Meurant, The Aesthetics of the Sacred: A Harmonic Geometry of Consciousness and Philosophy of Sacred Architecture (3rd ed.), The Opoutere Press (1989) ISBN 0-908809-02-6. (PhD thesis, Univ. of Auckland, 1984). Available at http://www.rmeurant.com/its/books.html

[11] R. C. Meurant, A New Order in Space – Aspects of a Three-fold Ordering of the Fundamental Symmetries of Empirical Space, as evidenced in the Platonic and Archimedean Polyhedra – Together with a Two-fold Extension of the Order to include the Regular and Semi-regular Tilings of the Planar Surface. Int. J. of Space Structures, Vol.6 No.1, Univ. of Surrey, Essex, 1991, 11–32. PDF 06, download: http://www.rmeurant.com/its/papers/polygon-1.html

[12] R. C. Meurant, The Myth of Perfection of the Platonic Solids. People and Physical Environment Research PAPER Conference on Myth Architecture History Writing, Univ. of Auckland 1991. PDF 07 in color, downloadable at: http://www.rmeurant.com/its/papers/polygon-1.html.

[13] R. C. Meurant, Towards a New Order of the Polyhedral Honeycombs: Part II: Who Dances with Whom? Information 2015: L. Li and T.-W. Kuo (eds.), Proceedings of The Seventh International Conference on Information, Taipei, Nov. 25–28, 2015, 369–373. PDF 61.

[14] R. C. Meurant, Towards a Meta-Order of the All-Space-Filling Polyhedral Honeycombs through the Mating of Primary Polyhedra. Information, Vol.19, No. 6(B), June 2016, 2111–2124. PDF 62.

[15] R. C. Meurant, Sequences of the All Space-filling Periodic Polyhedral Honeycombs. Information 2017. L. Li et al. (eds.), Proceedings of The Eighth International Conference on Information, Tokyo, May, 2017, 151–154. PDF 63.

[16] R. C. Meurant, Expansion Sequences and their Clusters of the All Space-filling Periodic Polyhedral Honeycombs. Information, Vol.20, No.10(A), Oct. 2017, 7345–7362. PDF 64.

[17] R. C. Meurant, Form and Counterform in the Periodic Polyhedral Honeycombs. Information 2018: L. Li et al. (eds.), Proc. of The 9th Int. Conf. on Information, Tokyo, Dec. 7–9, 2018, 51–56. PDF 65.

[18] R. C. Meurant, Towards a New Order of the Polyhedral Honeycombs: Part III: The Developed Metaorder, Form and Counterform. Information, Vol.22, No.1, Jan. 2019, 23–45. PDF 66.

[19] R. C. Meurant, A New 2.5D Schema of the Regular & Semi-regular Polyhedra and Tilings: Classes II and IV. Information, L. Li, R. Ashino, & C.-C. Hung (eds.), Proceedings of The Tenth International Conference on Information, Tokyo/Zoom, Mar. 6–7, 2021, 29–34. PDF 67.

[20] R. C. Meurant, A Novel 2.5D Schema of the Regular and Semi-regular Polytopes and their Sequences, with Analysis by Polytope and Surface Elements. Information Journal, International Information Institute, Vol.24, No.2, June 2021, pp.51–64. PDF 68.

[21] R. C. Meurant, Polytope Typology A: The separation of facial polytopes in the morphology of the regular and semi-regular polyhedra and tessellations. Information, Vol.28, No.1, March 2025, 5–21. PDF 71.

[22] R. C. Meurant, Polytope Typology B: Core–Shell, Core–Multi-shell, and Interlayer Configurations of the Polyhedra According to the Separation of Faces. Information, Vol.28, No.2, June 2025, 61–78. PDF 72.

[23] P. Zhang et al., Chiral separation and characterization of triazatruxene-based face-rotating polyhedra: the role of non-covalent facial interactions, Chemical Communications, 2018.

Supplementary Information: References [11–22] as PDFs (06, 07, 61–68, 71, 72), and PDF 73 of this paper, in color or greyscale, are downloadable from http://www.rmeurant.com/its/papers/polygon-1.html.

Robert C. Meurant □ B.Arch (Hons) (1978), and PhD in Architecture (1984), University of Auckland, New Zealand □ MA in Applied Linguistics (2007), University of New England, Australia □ Director Emeritus, Institute of Traditional Studies □ Taught in universities in New Zealand, the United States, and Korea □ Published 6 books, over 70 papers, presented papers in New Zealand, the U.S., the U.K., Japan, and Korea □ For many years, a director of the Science and Engineering Research Support Society (SERSC), Korea □ Research interests: sacred and traditional geometry, art, and architecture; the traditional philosophy of art; number and form; the polyhedra; structural morphology and geometry; deployable Space habitation and large-scale structures in microgravity, nanoarchitecture, applied linguistics □ ORCID iD: 0009–0001–4142–0699 ■ *NB.* A Nomenclature is provided below Table 3. ■